Improving Element-Boundary Alignment in All-Hex Meshes of Thin-Walled Solids by Side-Face Identification

Soji Yamakawa[1] and Kenji Shimada[2]

The Department of Mechanical Engineering,
Carnegie Mellon University,
[1]soji@andrew.cmu.edu
[2]shimada@cmu.edu

Abstract

This paper presents a new computational method for identifying side faces of thin-walled solids that can be excluded from the first step of conformal transformation from a tet mesh to an all-hex mesh. By excluding such side faces, all-hex meshes created by the conformal transformation method better align with the boundary of the side faces and tend to exhibit better scaled Jacobian quality. The proposed method first finds seeds of the candidate faces that may belong to the side faces. Then the candidate faces are grown across edges that have a low dihedral angle. Finally the candidate faces are retracted until no edge between a candidate face and non-candidate face has a low dihedral angle. Experimental results demonstrate clearly improvement of the element-boundary alignment and scaled Jacobian quality.

1. Introduction

This paper describes a method for automatically identifying side faces of thin-walled solids and improving boundary alignment of the hex elements created by the conformal mesh transformation method [1]. The proposed method first finds seed faces that are likely to be a part of a side face, which typically is a narrow face connecting two larger wall faces, by (1) calculating aspect ratio and depth-thickness ratio and (2) finding through holes. (See Section 3 for the definition of side- and wall-faces.) Then the seed faces are grown across edges that do not satisfy dihedral-angle

condition, detailed in Section 4. If the dihedral-angle condition cannot be satisfied even after growing the seed faces, seed faces are retracted until all the boundaries between seed faces and non-seed faces satisfy the dihedral-angle condition. The final remaining seed faces are considered the side faces.

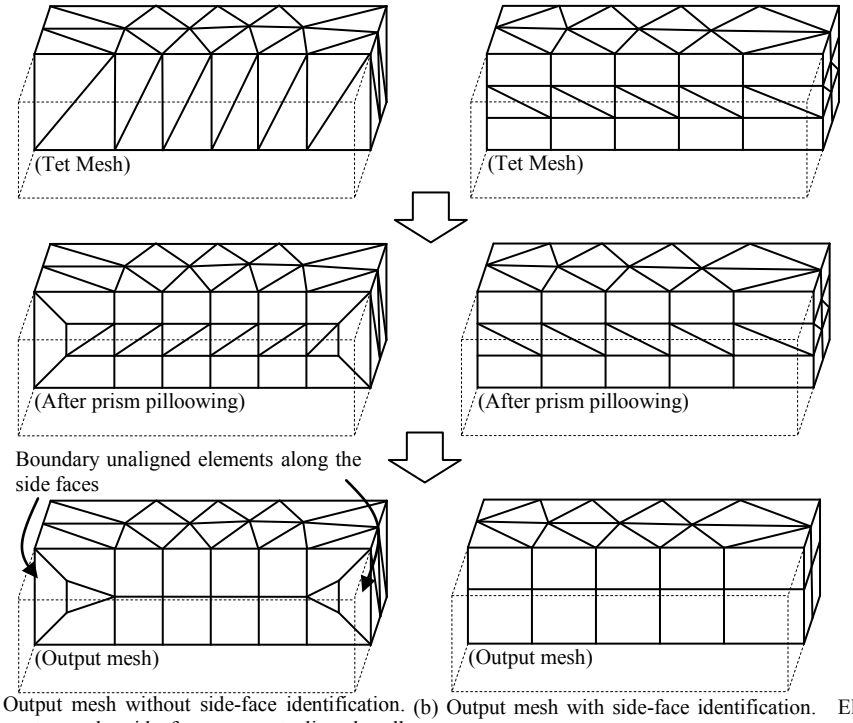

(a) Output mesh without side-face identification. Elements on the side faces are not aligned well with the boundary

(b) Output mesh with side-face identification. Elements on the side faces aligns well with the boundary.

Fig. 1. Effect of the side-face identification on the alignment

While the previous conformal-transformation method [1] creates an all-hex mesh of thin-walled solids, in which most elements are aligned with the boundary, the method creates elements that do not align the boundary in the region near the side faces. The new method automatically identifies side faces of the input geometry and improves the boundary alignment near such faces. This method is useful for the applications that are sensitive to the alignment of the elements such as a flow simulation of the injection-molding process.

The conformal-transformation method creates an all-hex mesh in three steps: (1) prism-tet mesh generation, (2) conformal transformation, and (3) mid-point subdivision. In the first step, an all-tetrahedral mesh of the input geometry is created and then, a layer of prism elements is inserted on

the mesh boundary (prism pillowing). The second step applies a sequence of topological transformations, detailed in [1], to reduce the number of tet elements and increase the number of hex elements. Since the topological transformations maintain the mesh conformity without the use of pyramid elements, every element in the mesh can be subdivided into all-hex elements with simple mid-point subdivision templates without losing the mesh conformity in Step (3).

Among these steps, the first step has the most significant influence on the alignment of the elements. The original conformal-transformation method inserts a layer of prism elements all over the boundary of the mesh as shown in Fig. 1 (a). After applying topological transformations, most of the tet elements are collapsed. The prism elements along the side faces, however, are not aligned well with the boundary as shown in Fig. 1 (b).

The boundary alignment can be improved by not inserting prism elements on the side faces as shown in Fig. 1 (c). If all of the tet elements are collapsed, prism elements are almost perfectly aligned with the wall faces.

When a high-quality all-hex mesh of a thin-walled solid is necessary, the model typically needs to be de-featured first and then decomposed into simpler map-meshable or sweep-meshable geometries, which then are meshed and merged together. Although the conformal-transformation method still requires the de-featuring process, it creates an adequate-quality mesh without going through manual geometry decomposition. The proposed method further improves the element boundary alignment of the output mesh by identifying side faces and avoids inserting prism elements in the first step of the conformal-transformation method.

2. Previous Work

Despite numerous attempts, none of the previously published techniques can automatically create an adequate quality all-hex mesh of an arbitrary geometry. When the input geometry is chunky and de-featured, grid-based and octree-based methods sometimes yield an adequate-quality all-hex mesh [2-12]. Orientation of the elements in meshes created by these types of methods is constrained by the original grid orientation, and therefore elements are not aligned well with the boundary. For better boundary alignment, a method for inserting a sheet of hex elements on the boundary of a grid-based or octree-based mesh has been introduced [13]. Although this technique solves the boundary-alignment problem of the exterior elements, the orientation of the interior elements is still constrained by the original grid orientation. The grid-based and octree-based meth-

ods do not perform well when the input geometry is thin-walled, and when the boundary alignment significantly influences the solution accuracy.

When it is necessary to create a high-quality all-hex mesh in which the elements are aligned with the boundary, the input geometry needs to be first de-featured, and then manually decomposed into simpler geometries each of which can be map-meshed or sweep-meshed. Although the outcome of this manual meshing would yield a high-quality mesh, it requires substantial manual intervention and may not be feasible all the time.

The conformal-transformation method creates a reasonably good-quality all-hex mesh of thin-walled solids, in which the elements are well aligned with the boundary [1]. The boundary alignment achieved by the conformal-transformation method alone tends to be better than grid- and octree-based methods. A mesh created by a typical grid- or octree-based method plus hex pillowing tends to have boundary unaligned interior elements because the orientation of the interior elements is significantly limited by the grid orientation as shown in Fig. 2 (a). On the other hand, the conformal-transformation method creates more boundary aligned interior elements than the grid- or octree-based methods since boundary unaligned interior elements are mostly collapsed by the topological transformations as shown in Fig. 2 (b). The conformal-transformation method, however, still creates boundary unaligned elements near the side faces. The goal of the proposed method is identifying side faces and improving boundary alignment near such side faces as shown in Fig. 2 (c).

The proposed method pertains to feature-identification techniques. In the past, feature identification techniques mainly targeted feature-edge identification and preservation [11, 14-17] and geometry simplification [18]. None of the existing techniques is directly applicable to the identification of side faces for the purpose of improved element boundary alignment.

Yin et al. have presented a method for identifying thin sections of the input volume [19]. Thin sections are meshed with prism elements and the rest with tetrahedral elements. Since triangular faces of the tetrahedral elements are exposed to the quadrilateral faces of the prism elements, the output mesh is a non-conformal prism-tetrahedral mesh. The advantage of the conformal-transformation method over Yin et al.'s method is (1) the mesh stays conformal throughout the process, and (2) it does not require an explicit separation of the volume into thin sections and non-thin sections.

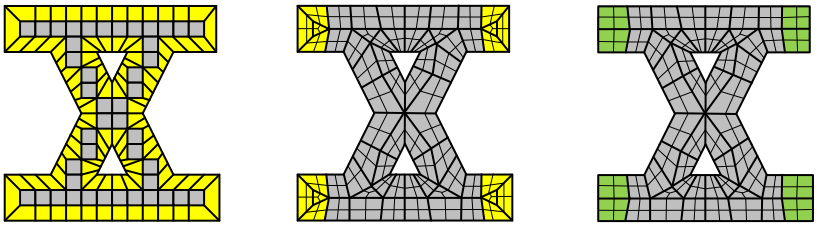

(a) A typical mesh created by the 2D version of grid- or octree-based method plus surface element pillowing.

(b) A typical mesh created by the 2D version of conformal transformation method. Interior elements are better aligned with the boundary.

(c) Element-boundary alignment and quality improves near side faces by the proposed method

Fig. 2. Comparison of typical meshes created by the grid- or octree-based method plus surface element pillowing vs. the conformal transformation method.

3. Definition of a Side Face

A side face is a face of a thin-walled solid that connects multiple wall faces. Side faces are typically narrow and connecting a pair of larger wall faces. Shaded faces in Fig. 3 are side faces of a thin rectangular solid.

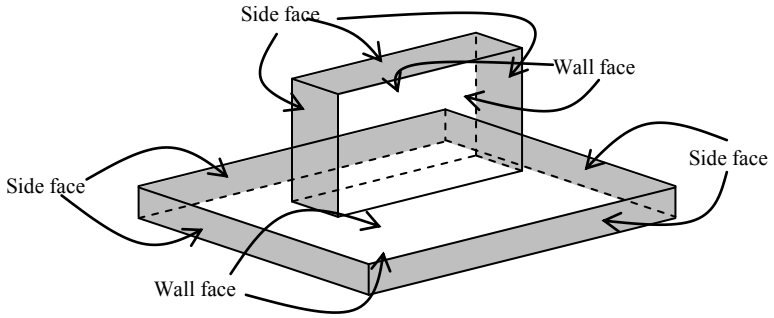

Fig. 3. Side and wall faces of a thin rectangular solid

The proposed method calculates three dimensions, *depth*, *thickness*, and *length* for identifying side faces. *Depth, d,* is defined at a point on a face as the length of a ray shot from the point on the surface to the opposite direction of the normal vector at the point that extends until it hits another face. The direction of the ray needs to be corrected when it intersect with a face that is a direct neighbor of the face from which the ray is originated because it is likely that the side face is not perpendicular to the wall face. In this case, the corrected ray direction, $\mathbf{r}'$, is calculated as:

$$\mathbf{r}' = \mathbf{r} - \mathbf{n}(\mathbf{n} \cdot \mathbf{r}),$$

where $\mathbf{r}$ is the original ray direction, and $\mathbf{n}$ is the normal of the boundary surface where the original ray intersects with.

Thickness is defined as an average distance over the side face between the two wall faces, and *length* is defined as a half of the total length of the edges of a side face that are shared by wall faces.

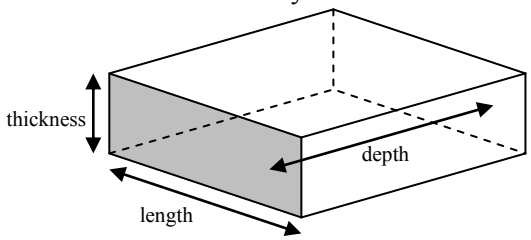

Fig. 4. Thickness, length, and depth of a side face

Faces need to be classified into side faces and wall faces to calculate thickness and length. Such classifications, however, are not known up-front, and thickness and length thus can only be calculated approximately.

For a set of faces, *thickness* and *length* can be approximated as follows. Let L and A be the total length of the outer perimeter and the total area of the set of faces, respectively. If the set of faces is long and thin, it is approximately similar to a rectangle as shown in Fig. 5.

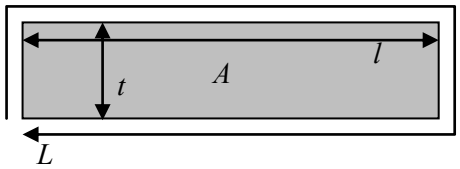

Fig. 5. Approximating a set of faces with a rectangle

The relation between A, L, and thickness t, and length l are:

$$A = lt \tag{1}$$

$$L = 2(l + t), \tag{2}$$

which leads to:

$$2t^2 - Lt + 2A = 0. \tag{3}$$

Thickness t becomes imaginary if the set of faces is more similar to a circle than a square, in which case it is sufficient to consider it a square for the purpose. Also, since l is longer dimension of the rectangle, one of the roots of (3) is dropped. Finally, t and l are solved as:

$$t = \begin{cases} \frac{L-\sqrt{L^2-16A}}{4} & \text{if } L^2 > 16A \\ L/4 & \text{otherwise} \end{cases} \tag{4}$$

$$l = A/t \tag{5}$$

If a set of faces are connecting only two other faces, it can be either a through hole or an extrusion, and the length, l_h, and thickness, t_h, must be calculated differently. Since such a set of faces is closed, total length of the outer perimeter is shorter than an open set of faces as shown in Fig. 6.

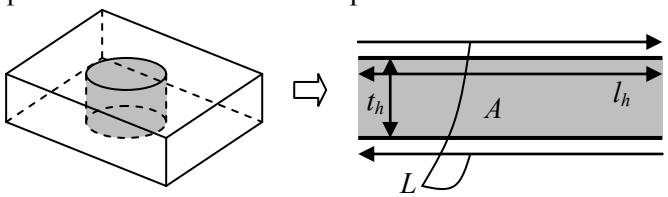

Fig. 6. Approximating a through hole with a rectangle

The relation between L and l_h thus becomes:

$$L = 2l_h. \quad (6)$$

By solving Equations (1) and (6), l_h and t_h for a through hole can be calculated as:

$$t_h = \frac{2A}{L}, \quad (7)$$

$$l_h = L/2. \quad (8)$$

4. Side Faces that can be Excluded from Prism Pillowing

The goal of the proposed method is finding side faces and excluding them from prism pillowing, which is a part of the first step of the conformal-transformation method. Not-all side faces, however, can be excluded from prism pillowing. The side face that is excluded from prism pillowing must satisfy one condition: the outer perimeter edges must be either convex or connected to another face that is also excluded.

A prism element placed next to a face that is excluded from prism pillowing needs to have at least one edge extended along the excluded face as shown in Fig. 7, or the element will not be connected to the interior elements. If part of the outer perimeter of the excluded face is concave, a prism element on the concave edge will have inverted or negative Jacobian as shown in Fig. 8.

In fact, the outer perimeter must not only be convex but also have greater than a certain dihedral angle to avoid sacrificing scaled-Jacobian quality. In theory, the threshold of the dihedral angle is 60 degrees because scaled Jacobian does not change if one element occupies a 60-degree (120-degree interior) corner or if two elements share the same corner. If the dihedral angle of an edge is exactly 60 degrees, excluding a face on such an edge from prism pillowing makes no change in scaled Jacobian, as

shown in Fig. 9. If the dihedral angle is greater than 60 degrees, excluding one side of the edge from prism pillowing improves the scaled Jacobian. Or, if the dihedral angle is less than 60 degree, excluding one side of the edge adversely affects the scaled Jacobian.

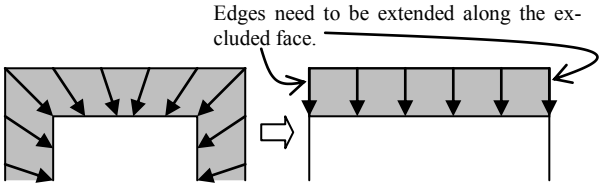

Fig. 7. Improving element alignment and scaled Jacobian together by excluding side faces from prism pillowing (shaded elements are prism elements)

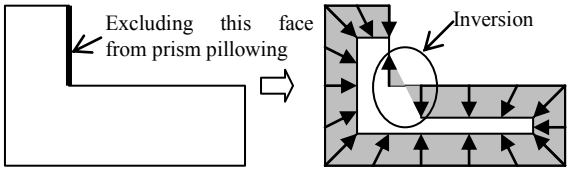

Fig. 8. Concave edge on the outer perimeter of an excluded face will cause an inverted (negative Jacobian) prism

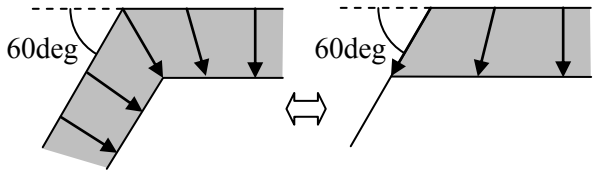

Fig. 9. Excluding a face on 60-degree dihedral angle from prism pillowing makes no change in scaled Jacobian

Dihedral angle on the outer perimeter of side faces varies along the perimeter in a real model. Applying 60 degree minimum dihedral-angle threshold is too restrictive, according to the experiments. The experiments conducted in this research have shown that 40 to 45 degree threshold gives a reasonably good result. For the best result, however, this threshold needs to be given by the user.

5. Side-Face Identification

The proposed method takes three thresholds: (1) depth-thickness ratio threshold s_{dt}, (2) aspect-ratio threshold s_{ar}, and (3) dihedral angle threshold s_{dha}, to identify side faces that can be excluded from prism-pillowing and improves the alignment of hex elements.

The method finds such side faces in three major steps:

(1) finding candidate seed faces,
(2) growing candidate faces so that concave candidate-face boundary edges decrease, and
(3) retracting candidate faces so that all of the concave candidate-face boundary edges disappear.

In the first step, the proposed method identifies thin faces and through holes. A face is considered thin if the following conditions are satisified:

Condition 1: $l/t > s_{ar}$, and

Condition 2: $\min(d)/t > s_{dt}$,

where l and t are *length* and *thickness* calculated by Equations (4) and (5), and $\min(d)$ is the minimum depth of the face. Condition 1 tests if the face has a higher aspect ratio than the given threshold, and Condition 2 makes sure the wall is tall compared to the thickness.

Through holes can be identified by finding a set of faces each of which is connected to two common faces, and the boundary edges of the set of faces are all convex. This condition alone will capture both shaded faces in Figs. 10 (a) and (b). However, for the purpose of the proposed method, shaded face in Fig. 10 (a) should not be identified as a side face since it is one of the wall faces. To prevent wall faces from being identified as a side face, the proposed method applies an additional condition for a through hole:

Condition 3 $\min(d)/t_h > s_{dt}$,

where t_h is the thickness of the through hole calculated by Equation (7). Note that Condition 3 is tested per set of the candidate faces. This prevents false identification of a thin face that is a part of and smoothly connected to a larger face.

In the second step, the proposed method grows the side-face candidates across low-dihedral-angle edges on the boundary between candidate- and non-candidate- faces. If a non-candidate face shares a low-dihedral-angle edge with a candidate face, and if the non-candidate face satisfies Condition 2, the non-candidate face is added to the list of side-face candidates. This process is repeated until the side-face candidates no longer grow.

In the third step, a face in the set of side-face candidates is removed from the set if one of the edges of the face has lower dihedral angle than s_{dha} and a non-candidate face is connected to the face across the edge. This process is repeated until no more face can be removed from the side-face candidates.

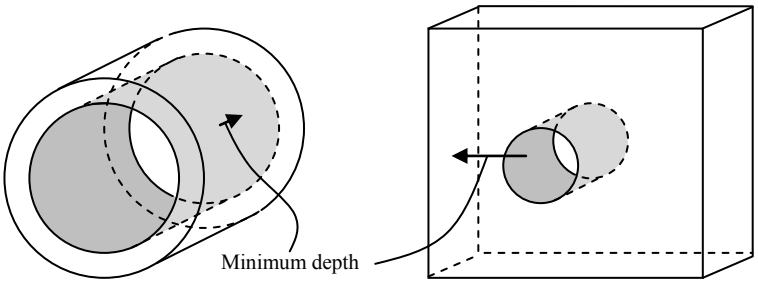

(a) A through hole surface that is a part of wall faces

(b) A through hole surface that is a part of side faces

Fig. 10. Through hole that connects two common faces

6. Effect of Geometry Simplification

The proposed method assumes that the input geometry is reasonably simplified. The simplification process is a prerequisite for almost any types of meshing algorithm, or the output-mesh quality can never be good. In particular, un-removed fillets substantially increase the difficulty of the side-face identification.

For example, if corners of a side-face are filleted as shown in Fig. 11 (a), the faces are not identified as a side face since the dihedral angle between the side faces (shaded) and wall faces (white) is zero. While concave fillets are typically for avoiding stress concentration, these types of convex fillets are in many cases for aesthetic purposes and do not make notable difference in the analysis.

If the fillets are removed, the proposed method is able to identify shaded faces in Fig. 11 (b) as side faces, and the mesh quality, in terms of both the boundary alignment and the scaled Jacobian, can substantially be improved.

If corners of a through hole is filleted as shown in Fig. 12, the proposed method cannot identify the hole surfaces as side walls because none of the faces connects two wall faces. These faces can easily be identified as side faces if the fillet on the corners of the hole is removed.

Although some CAD packages keep track of the fillet surfaces and are able to remove most of them automatically with a push of a button, some of such fillets cannot automatically be removed due to feature dependencies and attributes lost in process of the modeling.

Dealing with fillets has been one of the major challenges of mesh generation, not only for the proposed method since it obscures the boundary between features. Also a fillet surface tends to be thinner than the desired

edge length, and often the mesh needs to include a sequence of edges that lie on the centroid of the fillet surface, although such constraint cannot easily be calculated especially where multiple fillets meet. The development of a method that can automatically identify and remove fillets would be a substantial contribution to the meshing research.

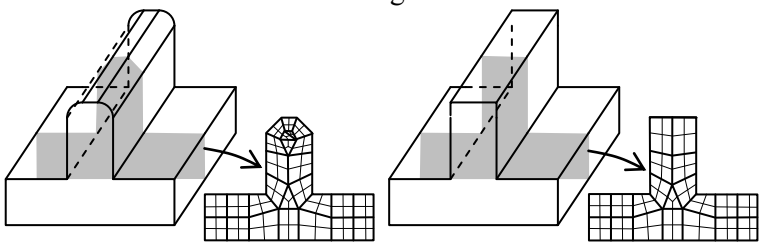

(a) Relatively low-quality elements will remain if fillets are left unremoved.

(b) Alignment and quality of elements improve if fillets are removed.

Fig. 11. Effect of unremoved fillets

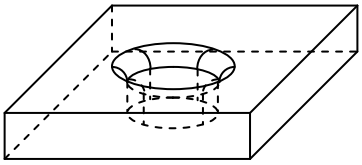

Fig. 12. Fillet on a corner of the through hole makes side-face identification more difficult

7. Experimental Results

The experiments conducted in this research have shown the effectiveness of the proposed method. For these examples, threshold values of s_{dt}=1.0, s_{ar}=3.0, and s_{dha}=40 degree have been used.

Fig. 13 (a) shows a tet mesh of a lid model that is used as the initial mesh for the conformal-transformation method. The faces identified as side faces by the proposed method are highlighted. Fig. 13 (b) shows some cross-sections of an all-hex mesh created by the conformal-transformation method without using side-face identification. The same cross-sections of an all-hex mesh created with side-face identification are shown in Fig. 13 (c). The element-boundary alignment clearly improves with the proposed side-face identification.

The proposed method also improves the scaled Jacobian quality. Without the side-face identification, the peak of the scaled Jacobian histo-

gram is near 0.7. With the side-face identification, the peak is shifted to near 0.8 as shown in Fig. 16.

Fig. 14 (a) shows a tet mesh of a plastic cover that is used as the initial mesh for the conformal-transformation method. The faces identified as side faces by the proposed method are highlighted. Fig. 14 (b) shows some cross-sections of an all-hex mesh created by the conformal-transformation method without the side-face identification. The same cross-sections of an all-hex mesh created with the side-face identification are shown in Fig. 14 (c). The element-boundary alignment clearly improves with the side-face identification.

The peak of scaled Jacobian histogram is near 0.8 without side-face identification. With side-face identification, the peak jumps to near 0.9.

Fig. 15 (a) shows a tet mesh of an aorta-artery model that is used as the initial mesh for the conformal-transformation method. The faces identified as side faces by the proposed method are highlighted. Fig. 15 (b) and (c) show all-hex meshes with and without applying the proposed method, respectively. Fig. 15 (c) clearly shows that the proposed method improves the element-boundary alignment on the side faces. Fig. 18 indicates that the peak of the scaled Jacobian histogram shifts from 0.65 to 0.7 with the side-face identification.

These results suggest that the proposed method is effective in improving the element-boundary alignment on the side faces and also tends to improve scaled Jacobian quality.

8. Conclusion

This paper has presented a new method for identifying side-faces of a thin-walled solid that can be excluded from prism-pillowing in the first step of the conformal-transformation method. The method searches the side faces based on the high aspect ratio faces and through holes. The candidate side faces are once grown across low dihedral-angle edges, and then retracted until no boundary edge between candidate face and non-candidate has low dihedral-angle. The effect of the method is the improvement of the element-boundary alignment and scaled Jacobian quality. The experimental results show that the proposed method effectively improves the quality of all-hex meshes created by the conformal-transformation method.

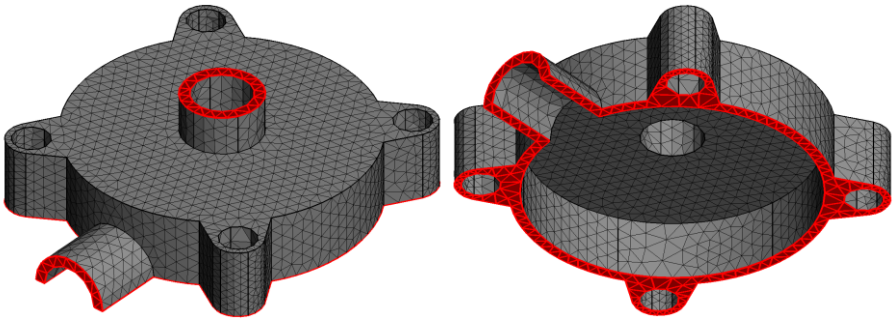

(a) A tet mesh of a lid model used as the initial mesh for the conformal-transformation method. Faces identifies as side faces are highlighted.

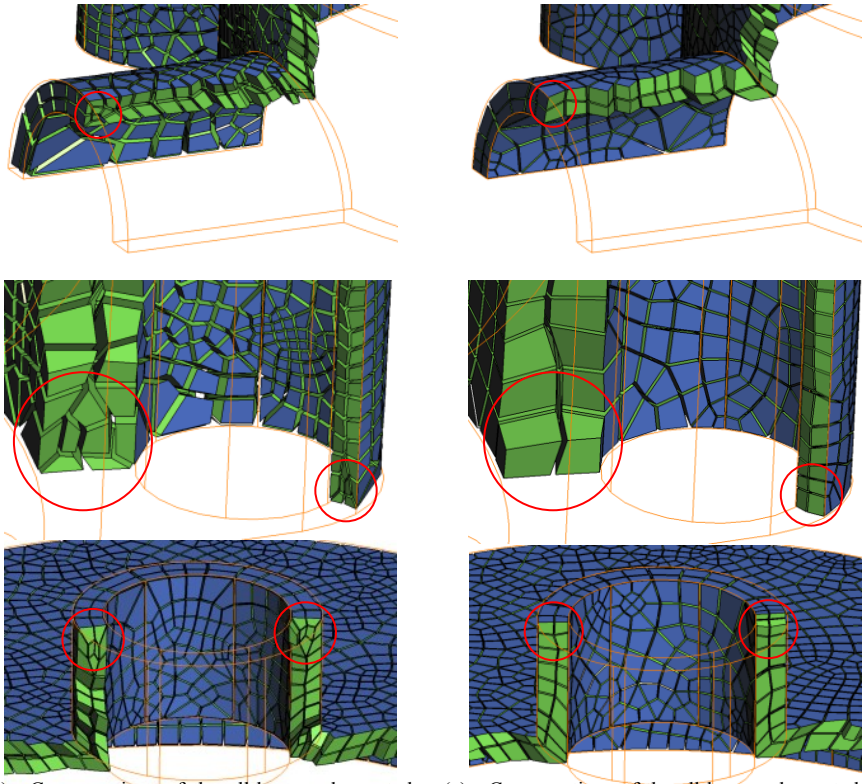

(b) Cross sections of the all-hex mesh created by the conformal transformation method without side-face identification. (23,821 nodes and 15,146 hexes)

(c) Cross sections of the all-hex mesh created by the conformal transformation method with side-face identification. Elements in the circles are clearly better aligned with the boundary. (22,592 nodes and 13,798 hexes)

Fig. 13. All-hex meshes of a lid model

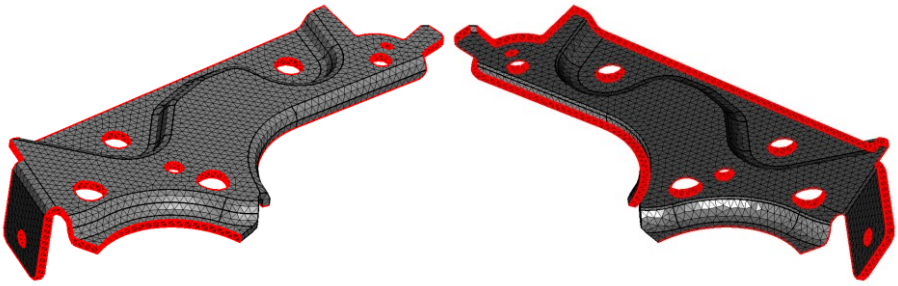

(a) A tet mesh of a plastic cover used as the initial mesh of the conformal-transformation method. The faces identified as side faces are highlighted.

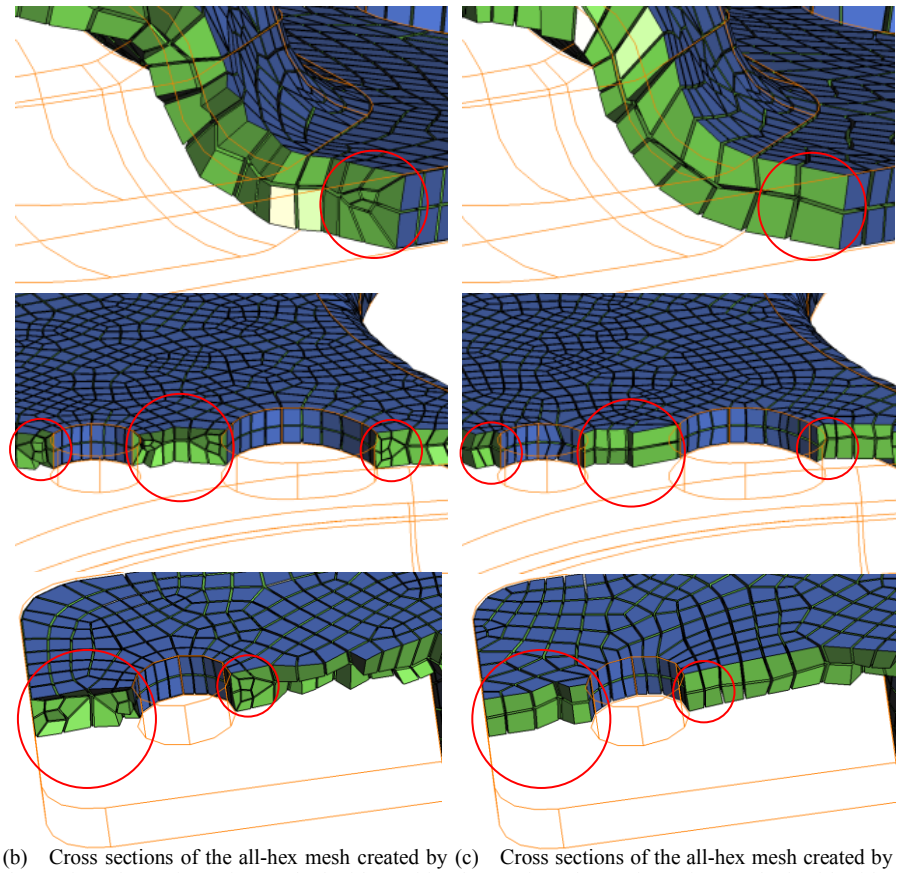

(b) Cross sections of the all-hex mesh created by the conformal transformation method without side-face identification.
(24,920 nodes and 15,976 hexes)

(c) Cross sections of the all-hex mesh created by the conformal transformation method with side-face identification. Elements in the circles are clearly better aligned with the boundary.
(22,362 nodes and 13,114 hexes)

Fig. 14. All-hex meshes of a plastic-cover model

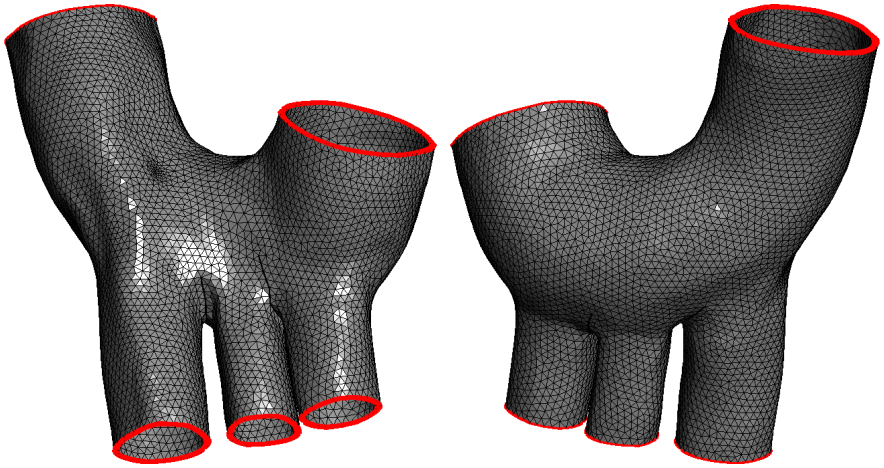

(a) A tet mesh of an aorta-artery model. The faces identified as side faces are highlighted.

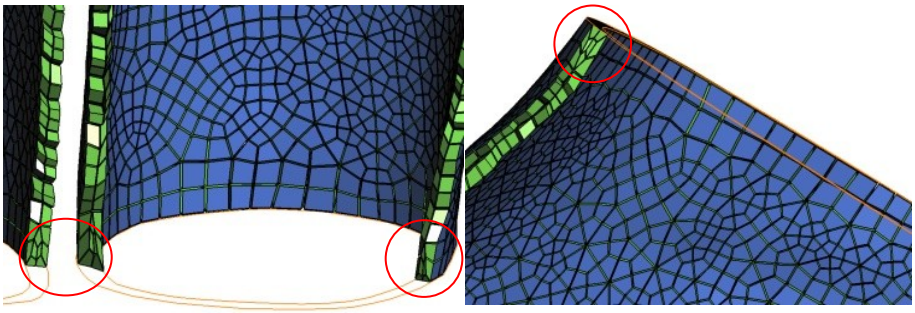

(b) Cross sections of the all-hex mesh created by the conformal transformation method without side-face identification. (95,357 nodes and 59,222 hex elements)

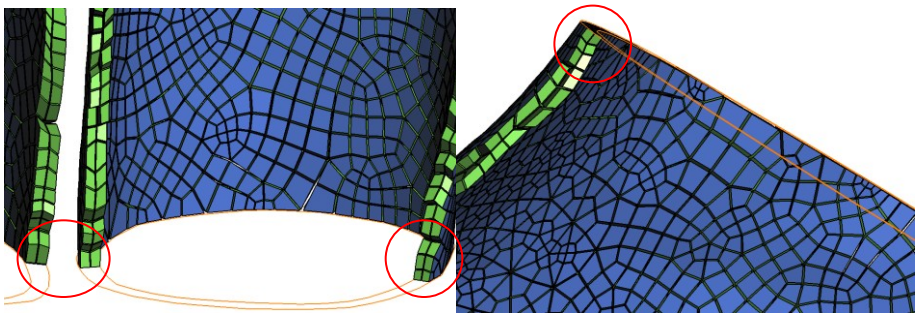

(c) Cross sections of the all-hex mesh created by the conformal transformation method with side-face identification. (90,835 nodes and 55,584 hex elements)

Fig. 15. All-hex meshes of an aorta-artery model

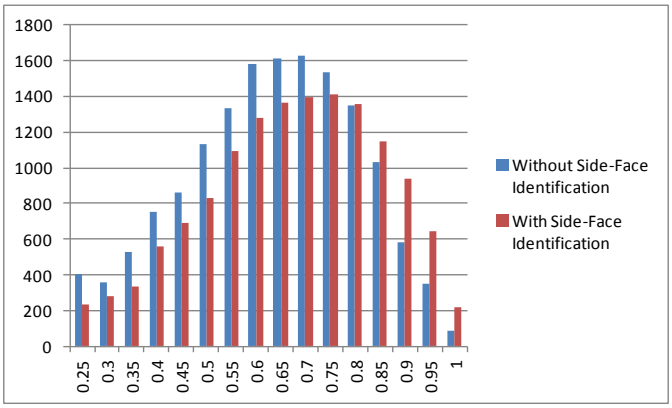

Fig. 16. Histograms of scaled Jacobian values of the all-hex meshes of the lid model.

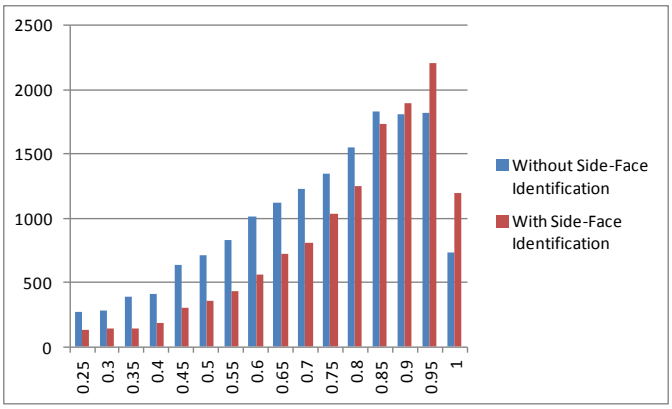

Fig. 17. Histograms of scaled Jacobian values of the all-hex meshes of the plastic-cover model.

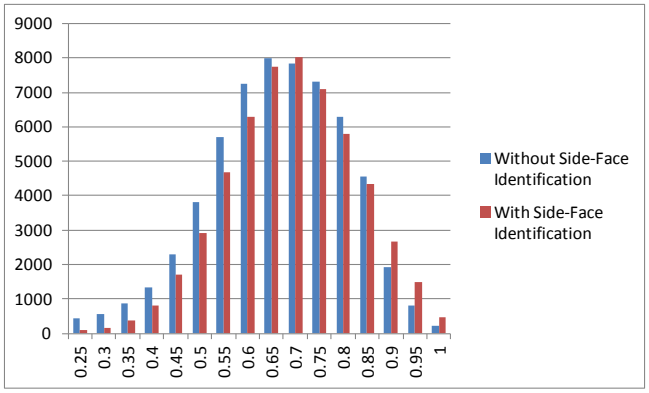

Fig. 18. Histograms of scaled Jacobian values of the all-hex meshes of the aorta-artery model

References

1. S. Yamakawa and K. Shimada, "Automatic All-Hexahedral Mesh Generation of Thin-Walled Solids via a Conformal Pyramid-less Hexahedral, Prism, and Tetrahedral Mixed Mesh," Proceedings of *20th Internation Meshing Roundtable*, Paris, France, pp. 125-141, 2011.
2. R. Schneiders, "A Grid-based Algorithm for the Generation of Hexahedral Element Meshes," *Engineering with Computers,* vol. 12, pp. 168-177, 1996.
3. N. Chiba, I. Nishigaki, Y. Yamashita, C. Takizawa, and K. Fujishiro, "A Flexible Automatic Hexahedral Mesh Generation by Boundary-Fit Method," *Computer Methods in Applied Mechanics and Engineering,* vol. 161, pp. 145-154, 1998.
4. H. Li and G. Cheng, "New Method for Graded Mesh Generation of All Hexahedral Finite Elements," *Computers and Structures,* vol. 76, pp. 729-740, 2000.
5. D.-Y. Kwak and Y.-T. Im, "Remeshing for Metal Forming Simulations-Part II: Three-Dimensional Hexahedral Mesh Generation," *International Journal for Numerical Methods in Engineering,* vol. 53, pp. 2501-2528, 2002.
6. M. Hariya, I. Nishigaki, I. Kataoka, and Y. Hiro, "Automatic Hexahedral Mesh Generation with Feature Line Extraction," Proceedings of *15th International Meshing Roundtable*, Birmingham, AL, pp. 453-467, 2006.
7. S. J. Owen and J. F. Shepherd, "Embedding Features in a Cartesian Grid," Proceedings of *18th International Meshing Roundtable*, Salt Lake City, UT, pp. 117-138, 2009.
8. R. Schneiders, R. Schindler, and F. Weiler, "Octree-based Generation of Hexahedral Element Meshes," Proceedings of *5th International Meshing Roundtable*, Pittsburgh, PA, pp. 205-215, 1996.
9. L. Maréchal, "A New Approach to Octree-Based Hexahedral Meshing," Proceedings of *10th International Meshing Roundtable*, Newport Beach, CA, pp. 209-221, 2001.
10. L. Maréchal, "Advances in Octree-Based All-Hexahedral Mesh Generation: Handling Sharp Features," Proceedings of *18th International Meshing Roundtable*, Salt Lake City, UT, pp. 65-85, 2009.
11. J. Qian and Y. Zhang, "Sharp Feature Preservation in Octree-Based Hexahedral Mesh Generation for CAD Assembly Models," Proceedings of *19th International Meshing Roundtable*, Chattanooga, TN, pp. 243-262, 2010.

12. J. Gregson, A. Sheffer, and E. Zhang, "All-Hex Mesh Generation via Volumetric PolyCube Deformation," *Computer Graphics Forum,* vol. 30, pp. 1407–1416, 2011.
13. K. Merkley, C. Ernst, J. F. Shepherd, and M. J. Borden, "Methods and Applications of Generalized Sheet Insertion for Hexahedral Meshing," Proceedings of *16th International Meshing Roundtable*, Seattle, WA, pp. 233-250, 2007.
14. S. Gumhold, X. Wang, and R. MacLeod, "Feature Extraction from Point Clouds," Proceedings of *10th International Meshing Roundtable*, Newport Beach, CA, pp. 293-305, 2001.
15. M. Nomura and N. Hamada, "Feature Edge Extraction from 3D Triangular Meshes Using a Thinning Algorithm," Proceedings of *SPIE - Vision Geometry X*, San Diego, CA, pp. 34-41, 2001.
16. X. Jiao and M. T. Heath, "Overlaying Surface Meshes, Part II: Topology Preservation and Feature Detection," *International Journal on Computational Geometry and Applications,* vol. 14, pp. 403-419, 2004.
17. S. Yamakawa and K. Shimada, "Polygon Crawling: Feature-Edge Extraction from a General Polygonal Surface for Mesh Generation," Proceedings of *14th International Meshing Roundtable*, San Diego, CA, pp. 257-275, 2005.
18. J. Ribelles, P. Heckbert, M. Garland, T. Stahovich, and V. Srivastava, "Finding and Removing Features from Polyhedra," Proceedings of *ASME Design Automation Conference*, Pittsburgh PA, 2001.
19. L. Yin, X. Luo, and M. S. Shephard, "Identifying and Meshing Thin Sections of 3-d Curved Domains," Proceedings of *14th International Meshing Roundtable*, San Diego, CA, pp. 33-54, 2005.